EC
Journals.ASM.org

Hammondia hammondi Harbors Functional Orthologs of the Host-Modulating Effectors GRA15 and ROP16 but Is Distinguished from *Toxoplasma gondii* by a Unique Transcriptional Profile

Katelyn A. Walzer,[a] Gregory M. Wier,[a] Rachel A. Dam,[a] Ananth R. Srinivasan,[a] Adair L. Borges,[a] Elizabeth D. English,[a] Daland C. Herrmann,[b] Gereon Schares,[b] Jitender P. Dubey,[c] Jon P. Boyle[a]

Dietrich School of Arts and Sciences, Department of Biological Sciences, University of Pittsburgh, Pittsburgh, Pennsylvania, USA[a]; Federal Research Institute for Animal Health, Institute of Epidemiology, Greifswald—Isle of Riems, Germany[b]; Animal Parasitic Diseases Laboratory, Beltsville Agricultural Research Center, Agricultural Research Service, U.S. Department of Agriculture, Beltsville, Maryland, USA[c]

***Toxoplasma gondii* and its nearest extant relative, *Hammondia hammondi*, are phenotypically distinct despite their remarkable similarity in gene content, synteny, and functionality. To begin to identify genetic differences that might drive distinct infection phenotypes of *T. gondii* and *H. hammondi*, in the present study we (i) determined whether two known host-interacting proteins, dense granule protein 15 (GRA15) and rhoptry protein 16 (ROP16), were functionally conserved in *H. hammondi* and (ii) performed the first comparative transcriptional analysis of *H. hammondi* and *T. gondii* sporulated oocysts. We found that GRA15 and ROP16 from *H. hammondi* (HhGRA15 and HhROP16) modulate the host NF-κB and STAT6 pathways, respectively, when expressed heterologously in *T. gondii*. We also found the transcriptomes of *H. hammondi* and *T. gondii* to be highly distinct. Consistent with the spontaneous conversion of *H. hammondi* tachyzoites into bradyzoites both *in vitro* and *in vivo*, *H. hammondi* high-abundance transcripts are enriched for genes that are of greater abundance in *T. gondii* bradyzoites. We also identified genes that are of high transcript abundance in *H. hammondi* but are poorly expressed in multiple *T. gondii* life stages, suggesting that these genes are uniquely expressed in *H. hammondi*. Taken together, these data confirm the functional conservation of known *T. gondii* virulence effectors in *H. hammondi* and point to transcriptional differences as a potential source of the phenotypic differences between these species.**

Toxoplasma gondii is a highly successful intracellular parasite, having infected nearly one-third of the human population (1). A member of the phylum Apicomplexa, *T. gondii* is primarily asymptomatic in healthy adults, but it can cause severe disease *in utero* and in immunocompromised humans (2–5). In rare, but nonetheless important, cases, *T. gondii* can cause lethal toxoplasmosis in immunocompetent adults (6). Importantly, *T. gondii* can infect, and cause disease in, nearly all warm-blooded animals studied to date, including multiple bird species (7–9). Such a vast host range is rare, if not unprecedented, among the members of the Apicomplexa, but the molecular basis for this feature is currently unknown and likely to be driven by multiple genetic mechanisms.

T. gondii's closest extant relative is *Hammondia hammondi* (10, 11), a fellow coccidian that shares the same definitive host (5). To date *H. hammondi* has been isolated in the field from a variety of animals, including cats, rodents, goats, and roe deer (reviewed in reference 9). Experimentally, this parasite appears to have a more restricted host range than *T. gondii* (e.g., *H. hammondi* cannot infect avian species [5]), but in contrast to the extensive work carried out on *T. gondii* field isolates (12, 13), there is much less information from wild *H. hammondi* isolates to make a definitive conclusion about the host range of this parasite.

Laboratory mice are often used as experimental models for both *T. gondii* and *H. hammondi* (9) and highlight key phenotypic differences between the species. While highly virulent *T. gondii* infections can be initiated in mice by multiple life stages and infection routes (14, 15), *H. hammondi* infections in mice can be initiated only by oocysts and infections are often asymptomatic in wild-type, immunosuppressed, and interferon gamma knockout mice (9, 16). Importantly, *H. hammondi* tissue cysts, which are predominantly found in muscle (whereas *T. gondii* tissue cysts can be found in diverse mouse tissues, including the brain), are not directly infective to mice by any route (5, 9, 16). In fact, given their morphological and antigenic similarities (17), the difference in the ability to be transmitted between intermediate hosts is used to experimentally distinguish *T. gondii* from *H. hammondi* (16).

Recently, a few key effector genes have been identified in *T. gondii*. These include the secreted effectors rhoptry proteins 18 and 5 (TgROP18 and TgROP5), which underlie strain-specific differences in virulence between *T. gondii* strains (15, 18–23). In addition, ROP16 and dense granule protein 15 (GRA15) have less dramatic, but significant, effects on virulence in the mouse and also significantly alter host cell transcription (24–27). All of the aforementioned effectors are secreted into the host cell, where they alter innate immune signaling pathways (via STAT3/6 for ROP16 and NF-κB for GRA15).

Given their high degree of genetic similarity and genomic synteny (28), *T. gondii* and *H. hammondi* provide a unique opportunity for functional comparative genomics studies. We published a

Received 20 September 2014 **Accepted** 23 September 2014
Published ahead of print 3 October 2014
Address correspondence to Jon P. Boyle, boylej@pitt.edu.
Supplemental material for this article may be found at http://dx.doi.org/10.1128/EC.00215-14.

doi:10.1128/EC.00215-14

genomic sequence of a strain of *H. hammondi* isolated from a cat in Germany (HhCatGer041) and used this sequence to determine that the *H. hammondi* orthologs of the major *T. gondii* virulence factors TgROP5 and TgROP18 are functionally conserved in *H. hammondi* (28). Specifically, *H. hammondi* ROP18 and ROP5 could complement mouse virulence defects in select *T. gondii* strains (28). This indicates that the mere presence of virulence factors like ROP5 or ROP18 in the *H. hammondi* genome is not sufficient to explain the dramatic differences in mouse virulence between these two species. In the present study, we used the HhCatGer041 genome sequence to focus on the signaling effectors GRA15 and ROP16 (25, 27). Here we show that similar to HhROP5 and HhROP18, the *H. hammondi* GRA15 and ROP16 orthologs are functionally conserved. By "functionally conserved," we mean that when they are expressed in a relevant *T. gondii* background, they have effects on host cell signaling similar to those of their *T. gondii* orthologs. This provides further support for the idea that phenotypic differences between *T. gondii* and *H. hammondi* are not due to a lack of effector proteins that manipulate the host. Other mechanisms, including differences in the deployment of known effectors, the presence of currently uncharacterized "avirulence" effectors, and differences in developmental stage-switching and regulation, are more likely to underlie these phenotypic differences than gene content itself. In support of this, we also show that the transcriptomes of *H. hammondi* and *T. gondii* sporozoites are highly distinct and that their transcriptional profile differences may be a reflection of different mechanisms of growth regulation that are particularly apparent during both *in vitro* and *in vivo* growth (9).

MATERIALS AND METHODS

Parasite strains and maintenance. Parasites were used to infect monolayers of human foreskin fibroblasts (HFFs) grown at 37°C in 5% CO_2. HFFs were maintained in Dulbecco's modified Eagle medium with 10% fetal calf serum, 2 mM glutamine, and 50 μg/ml each of penicillin and streptomycin (cDMEM). RH, ME49, and CEP were used as representative type I, II, and III strains, respectively. For *H. hammondi* HhCatGer041 oocyst production, interferon gamma knockout mice were fed 10^4 *H. hammondi* oocysts and sacrificed 4 to 6 weeks later. For *T. gondii* VEG strain oocyst production, Swiss-Webster mice were used. Leg muscle (for *H. hammondi*) or brain (for *T. gondii*) tissues from infected mice were fed to young cats (10 to 20 weeks old), and feces were collected during days 7 to 11 postinfection. Unsporulated oocysts were isolated by sucrose flotation and allowed to sporulate at 4°C in 2% H_2SO_4 (9).

DNA isolation from *H. hammondi* oocysts. Sporulated oocysts (40 million to 80 million) were washed several times in Hanks' buffered saline solution (HBSS) and then treated with 10% bleach in phosphate-buffered saline (PBS) for 30 min. After removal of all traces of bleach by multiple washes and pelleting at 800 × *g* in a swinging bucket rotor, pellets were resuspended in 4 ml of HBSS in a 15-ml Falcon tube, and 1 g of sterile glass beads (710 to 1,180 μM; Sigma) was added. Parasites were vortexed on high speed for 30 s, cooled on wet ice for 30 s, and then vortexed for 30 s more. After the glass beads settled, the supernatant was removed and the glass beads were washed once with HBSS; this wash was combined with the supernatant and pelleted at 800 × *g*. DNA was isolated from this preparation, containing sporocysts that had been freed from the oocyst wall by mechanical disruption, using the DNAzol reagent according to the manufacturer's instructions. After resuspension of the DNA pellet in sterile water, it was phenol-chloroform-isoamyl alcohol (25:24:1; Sigma) extracted and reprecipitated. For two different preparations, 8 ng of DNA was then linearly amplified using the Genomiphi DNA amplification kit and ethanol precipitated. These preparations were used for PCR amplification (described below).

Dual-luciferase reporter assays. Putative promoters for genes derived from *T. gondii* and *H. hammondi* were compared to see how effective they were at driving firefly luciferase expression. Putative transcriptional start sites were determined using the *T. gondii* full-length cDNA database (http://fullmal.hgc.jp/index_tg_ajax.html [29]). For *GRA15*, the primers used for the *H. hammondi* promoter were 5′-CACCTAATAAAAATGCTCATGCACTGGT-3′ and 5′-ATCCATTGCTGAATGTTTGTTTACAAAGTG-3′ (930 bp upstream of the start codon). The primers used for the ME49 *GRA15* promoter (928 bp upstream of the start codon) were 5′-CACCTAATAAAAATGATCAATACACTGGT-3′ and 5′-ATCCATTGTTGAATGCTGGTTTACAAAGTG-3′. For *ROP16*, the primers used for the wild-type (WT) *H. hammondi* promoter were 5′-CACCTTCTGGGTAGATCAGCAATAAACA-3′ (865 bp upstream of the start codon) and 5′-ATCCATCTTGCGACAAACGTAATCACAG-3′. The primers used for the wild-type ME49 *ROP16* promoter (881 bp upstream of the start codon) were 5′-CACCCTCTGGGTAGAACAGCAATAGACA-3′ and 5′-ATCCATCTTGCGACAAACAAGATCACAG-3′. PCR fragments were directionally cloned into the Gateway entry vector pENTR/D-Topo (Invitrogen, Carlsbad, CA), and fragments in the proper orientation in the entry vector were recombined into a destination vector (pDestFire) containing firefly luciferase and a 3′ untranslated region (UTR) from *T. gondii* dihydrofolate reductase (DHFR) (30) using the Gateway LR Clonase II enzyme mix (Invitrogen) (31, 32). The forward primers included a CACC sequence required for directional cloning, while the reverse primers included an ATCCAT sequence which contains, in antisense orientation, the start codon and encodes an aspartic acid (both underlined in the primer sequences above).

We also used splicing-by-overlap extension (SOE) PCR to create chimeric ROP16 promoter luciferase constructs. To delete the 16 bp immediately preceding the putative transcriptional start site in the TgROP16 promoter, we used outer forward primer GGGGACAAGTTTGTACAAAAAAGCAGGCTCTCTGGGTAGAACAGCAATAGACA-3′ (where the underlined sequence represents a BP Clonase B1 recombination sequence) and reverse primer 5′-TGATAAATTTAATGAGTTGACTGCTCACGA-3′ to amplify the 5′ promoter sequence up to the 16 bp to be deleted. We used forward primer 5′-CATTAAATTTATCAAACATACACGATACCA-3′ and outer reverse primer 5′-GGGGACCACTTTGTACAAGAAAGCTGGGT*CATCCAT*CTTGCGACAAACAAGATCACAG (where the underlined sequence represents a BP Clonase B2 recombination sequence and the start codon and additional aspartic acid codon are shown in italics) to amplify the 3′ region of the putative promoter, starting just after the 16 bp to be deleted. Similarly, we inserted the 16 bp from the $TgROP16_{II}$ promoter into the HhROP16 promoter. To do this, we used outer forward primer 5′-GGGGACAAGTTTGTACAAAAAAGCAGGCTTTCTGGGTAGATCAGCAATAAACA-3′ (B1 recombination sequence underlined as above) and reverse primer 5′-CTTCGTTTCCCATTTTAGTTGACTGCTCACGACTCG-3′ (where the 16 bp from TgROP16 are underlined) to amplify the promoter sequence up to the location of the 16-bp HhROP16 deletion. We used forward primer 5′-AAAATGGGAAACGAAG CACTAAATTTATCAAACA-3′ (where the 16 bp to be inserted is underlined as above) and outer reverse primer 5′-GGGGACCACTTTGTACAAGAAAGCTGGGT*CATCCAT*CTTGCGACAAACGTAATCACAG-3′ (where the B2 site is underlined and the start and aspartic acid codons are in italics as above) to amplify the promoter sequence immediately after the 16-bp HhROP16 deletion. Gel-purified PCR products were used in SOE PCRs with only the relevant outer forward and outer reverse primers for both TgROP16 deletion constructs and HhROP15 insertion constructs, and products were sequentially cloned into pDONR221 and pDestFire using BP and LR cloning reactions as described above. The additional nucleotide after the start and aspartic acid codons in the outer reverse primers is necessary for cloning the fragment in frame with the luciferase gene when using BP cloning for the first step in Gateway cloning. For direct comparison to the insertion and deletion promoter constructs, we also generated wild-type TgROP16 and HhROP16 promoter constructs using the outer forward

and outer reverse primers, followed by an identical Gateway cloning regimen.

For luciferase assays, constructs were transfected into 15 million to 20 million parasites of the ME49 strain (between 50 and 70 μg) along with 20 μg of a vector containing *Renilla* luciferase driven by the *TUB1* promoter, used to normalize for the efficiency of plasmid uptake by parasites in different experiments (32, 33). Parasites were harvested and lysed 24 h after transfection. Firefly and *Renilla* luciferase levels were measured using a dual-luciferase reporter assay system (Promega).

GRA15 cloning and characterization. The *H. hammondi* GRA15 coding region plus 930 bp upstream of the start codon was amplified via PCR (forward, 5′-CACCTAATAAAAATGCTCATGCACTGGT-3′; reverse, 5′-CTACGCGTAGTCCGGGACGTCGTACGGGTATGGAGTTACCGC TGATTGTGTGCC-3′). The CACC sequence was used for directional cloning into the pENTR/D-TOPO vector (Invitrogen), and the underlined sequence in the reverse primer encodes a hemagglutinin (HA) tag and contains a stop codon. The sequence was cloned using LR Clonase recombination with the p-ATT-GRA2 destination vector (28). The p-ATT-GRA2 vector with the GRA15 insert was transfected into RHΔ*HXGPRT*, and resistant parasites harboring the vector, which contains an *HXGPRT* minigene, were selected in mycophenolic acid and xanthine as described previously (34). Transgenic parasites were cloned by limiting dilution. Expression of the transgenic construct was validated using anti-HA immunofluorescence.

ROP16 cloning and characterization. Since the *H. hammondi ROP16* promoter (865 bp upstream of the predicted start codon) was not active in firefly luciferase reporter assays (see Results), the coding region was amplified using the following primers: forward, 5′-GTCCATGCAT ATGAA AGTGACCACGAAACGGCTT -3′, and reverse, 5′-CGTCCCATGGCTT CCGATGTGAATAAGGTTGGGTAGT-3′. For *T. gondii* ROP16 (from the type II strain ME49), we amplified the gene using the following primers: forward, 5′-GTCAATGCATATGAAAGTGACCACGAAAGGG CTTG, and reverse, 5′-CTGTCGTACGGGTACATCCGATGTGAAGAA AGTTCGGTAGT-3′. Underlined sites in the primer represent NsiI and NcoI sites, respectively, for HhROP16 and NsiI and BsiWI sites, respectively, for $TgROP16_{II}$. Digested PCR products were ligated into the pGra-HA-HXGPRT vector (15) in frame with a C-terminal HA tag and downstream of the constitutive GRA1 promoter (35). Plasmids were transfected into ME49Δ*HXGPRT*, and stable transfectants were selected with mycophenolic acid and xanthine and cloned as described above.

Immunofluorescence. Parasites were allowed to invade cell monolayers on circular 12-mm coverslips for 18 or 24 h. The cells were washed once with PBS before fixation. In most cases, the cells were fixed with 4% formaldehyde for 20 min, washed twice in PBS, and blocked in PBS supplemented with 5% bovine serum albumin (BSA) and 0.2% Triton X-100 for at least an hour. Coverslips were incubated with primary antibodies for 1 to 3 h or overnight and with fluorescent secondary antibodies for 1 h. Hoechst dye (2 μg/ml) was used for DNA visualization. Parasite strains expressing green fluorescent protein (GFP) were fixed in ice-cold methanol for 20 min. Additionally, the procedures for pSTAT6 and NF-κB staining differed from the above. For NF-κB detection, the cell monolayer was infected with parasites for 18 h, after which the cells were fixed with 3% formaldehyde for 20 min. The cells were washed twice in PBS and permeabilized with 100% ethanol for 20 min. The cells were then washed twice in PBS and blocked in PBS supplemented with 3% BSA and 5% fetal calf serum for at least an hour. The rest of the procedure followed the general protocol above. For signal quantification, 10 infected cells were chosen randomly from each coverslip and photographed with QED *InVivo* software (Media Cybernetics). Nuclear signal was quantified using ImageJ.

For pSTAT6 analysis, host cells seeded onto coverslips were serum starved overnight. The serum-starved monolayer was infected for 24 h, after which the cells were fixed with 4% formaldehyde for 20 min followed by ice-cold methanol for 5 min (25). The rest of the procedure followed the general protocol above. For signal quantification, 10 infected cells were chosen randomly from each coverslip and were photographed with AxioVision software (Carl Zeiss, Inc.). For each infected cell, the average nuclear pSTAT6 signal, as well as the cytoplasmic pSTAT6 signal, was quantified using ImageJ. For ROP16 nuclear localization, cells were infected for 4 h with either RHΔ*ROP16*:$TgROP16_{I\text{-}HA}$ or ME49:$HhROP16_{HA}$ at a multiplicity of infection of 10 or 8, respectively, and then fixed and stained for HA as described above. For each infection, nuclear staining was assessed qualitatively for 20 infected cells to determine the efficiency of nuclear localization. Antibodies used in this study include 3F10 (anti-HA; Roche), anti-TgSAG1 (GenWay), anti-P-Stat6 (phospho-Tyr641; Cell Signaling Technology), anti-NF-κB p65 (D14E12) XP (Cell Signaling Technology), and secondary fluorescent antibodies (Invitrogen). Monoclonal antibodies to ROP7 and GRA7 were kindly provided by Peter Bradley (UCLA) (36).

Microarray hybridizations of RNA from *H. hammondi* and *T. gondii* sporulated oocysts. Sporulated oocysts from *H. hammondi* HhGER041 and *T. gondii* VEG were produced as described above and sporulated in 2% sulfuric acid at 4°C. Sporulated oocysts of both species were kept at 4°C for ~20 days prior to RNA harvest. To isolate RNA, ~80 million oocysts per species were washed with HBSS and treated with 10% bleach, and sporocysts were released using glass beads as described above for DNA isolation. Sporulation efficiency was ~40% for both *T. gondii* and *H. hammondi* oocysts. Pellets were resuspended in TRIzol reagent (Invitrogen) by pipetting and passed serially through 25- and 27-gauge needles. Preparations were centrifuged for 1 min at 5,000 × *g*, supernatants were chloroform extracted, and RNA was precipitated according to the manufacturer's instructions. Pellets were resuspended in RNase-free water, extracted with phenol-chloroform-isoamyl alcohol (25:24:1), and reprecipitated with 0.7 volume of isopropanol in the presence of 0.3 M sodium acetate (pH 5.2). Pellets were washed with 75% ethanol and resuspended in RNase-free water. Samples were labeled for array hybridization using the Illumina TotalPrep RNA amplification kit (Applied Biosystems, Carlsbad, CA). Labeled cRNA samples were hybridized using *Toxoplasma* 169 chips (available through the University of Pennsylvania Genomics Core Facility) (37). Three separate RNA isolations were performed for each species and hybridized separately.

Microarray data analysis. To permit analysis of hybridization data for two species, custom Affymetrix chip description files (CDF) were generated that contained only probes that had perfect matches to sequences in the *T. gondii* VEG (ToxoDB) and *H. hammondi* HhGer041 genomes (28) using BLASTN (38). The expression module of the chip contains 11 probes for each of 8,058 *T. gondii* genes, and 6,294 of these genes had at least one probe that perfectly matched the *T. gondii* VEG and *H. hammondi* HhGer041 genomes. A custom script (written in Perl and available upon request) was written to generate the CDF file. Raw CEL files for the *H. hammondi* and *T. gondii* VEG oocyst hybridizations, as well as those for the complete life cycle hybridizations for *T. gondii* strain M4 (GEO accession number GSE32427 [39, 40]) were analyzed using the Affy package implemented in R statistical software (41), and all data were normalized ("constant" method) and $\log_2$ transformed using "median polishing" (42). To identify genes with significantly different abundances between species, we used Rank Products (43) with a false-discovery rate of 1/100 as implemented in the MeViewer Module of the TM4 microarray software suite (44). Genes were deemed to be significantly different in abundance if the adjusted *P* value was ≤0.01. Gene ontology (GO) analyses of differentially expressed transcripts were conducted with GeneMerge (45) as described previously (46). GO categories were deemed significantly enriched if they had adjusted *P* values of ≤0.05.

Using cluster analysis of transcripts of higher abundance in *H. hammondi* than in *T. gondii* VEG sporozoites along with the *T. gondii* M4 expression data set (39, 40), we identified two gene clusters of interest: (i) genes that were more highly expressed in *H. hammondi* than in *T. gondii* VEG oocysts that were poorly expressed in all of the life cycle stages in the *T. gondii* M4 data set ("Hh specific") and (ii) genes that were more highly expressed in *H. hammondi* than in *T. gondii* VEG oocysts that were up-

regulated during the tachyzoite-to-bradyzoite transition in the *T. gondii* M4 data set ("Hh-TgCyst-high"). To identify transcripts with these profiles in an unbiased way, the entire data set was analyzed using Pavlidis template matching (PTM) (47) implemented in TM4 using a *P* value threshold of 1×10^{-5} and setting either the "high" values to the maximum of 1 and the "low" values to a minimum of 0. Significant genes were subjected to GO analysis as described above.

Microarray and sequence data accession numbers. Raw data for gene expression analysis have been deposited in the Gene Expression Omnibus Database under accession number GSE61963. *H. hammondi* GRA15 and ROP16 gene sequences have been deposited in GenBank under accession numbers KM676011 and KM676012, respectively.

RESULTS

GRA15 from *H. hammondi* activates host cell NF-κB in *T. gondii*. In Europe and North America several distinct, clonal genotypes of *T. gondii* are recognized, including types I, II, III, and IV (48–50). These strain types have significant phenotypic differences during infections *in vivo* and *in vitro* (51), and strain types I, II, and III, at least, appear to have arisen from only a few recent natural genetic crosses (52). Type II strains of *T. gondii* activate significantly more NF-κB than type I and III strains, and this is driven by the type II allele of *TgGRA15* (27). The predicted *H. hammondi* GRA15 protein shares the most sequence identity with $TgGRA15_{I}$ and $TgGRA15_{III}$ (80 and 79%, respectively) and shares an 84-amino-acid insertion (relative to $TgGRA15_{II}$) with $TgGRA15_{I}$ and $TgGRA15_{III}$ (see Fig. S2 in the supplemental material). However, using the neighbor-joining method based on percent identity which does not count sequence gaps (Fig. 1A), HhGRA15 is most similar to $TgGRA15_{II}$, and this is reflected in the fact that HhGRA15 encodes the same amino acid as $TgGRA15_{II}$ at 3 of 6 sites with polymorphisms that are specific to $TgGRA15_{II}$, and conversely at none of the 4 polymorphisms specific to $TgGRA15_{III}$ (see Fig. S2).

We wanted to determine if HhGRA15, similar to its *T. gondii* type II strain ortholog, could activate the NF-κB pathway. Since to date no reliable *in vitro* culture system exists for *H. hammondi*, we used *T. gondii* as a surrogate for *H. hammondi*-derived constructs. We compared the promoter activities of *HhGRA15* and $TgGRA15_{II}$ and found that the *H. hammondi GRA15* promoter was active when expressed heterologously in *T. gondii* type II, though it was 4.6-fold ± 1.2-fold less active than the $TgGRA15_{II}$ promoter (Fig. 1B). We reasoned that the observed promoter activity for HhGRA15 was significant, in that it was ~6,000-fold above background levels (see Table S1 in the supplemental material). To determine if HhGRA15 was functional with respect to NF-κB activation, we complemented a type I *T. gondii* strain (RH, which does not significantly activate NF-κB [27]) with HA-tagged HhGRA15. Importantly, HhGRA15 protein was efficiently expressed (Fig. 1C) and colocalized with the dense granule marker GRA7, indicating that it is appropriately trafficked in *T. gondii* (Fig. 1D). As expected, nuclear NF-κB p65 levels in *T. gondii* type I-infected cells were nearly equal to background, while levels in *T. gondii* type II-infected cells were more than 100 times greater (Fig. 2A and B). *T. gondii* type I expressing HhGRA15 also activated the translocation of NF-κB p65 to the host cell nucleus at a level 100 times greater than *T. gondii* type I (Fig. 2A and B). This activation by *H. hammondi* GRA15 was similar to that of *T. gondii* type II, suggesting that *H. hammondi* GRA15 acts similarly to *T. gondii* type II GRA15 to effect downstream induction of inflammatory and anti-apoptotic pathways via NF-κB activation (27).

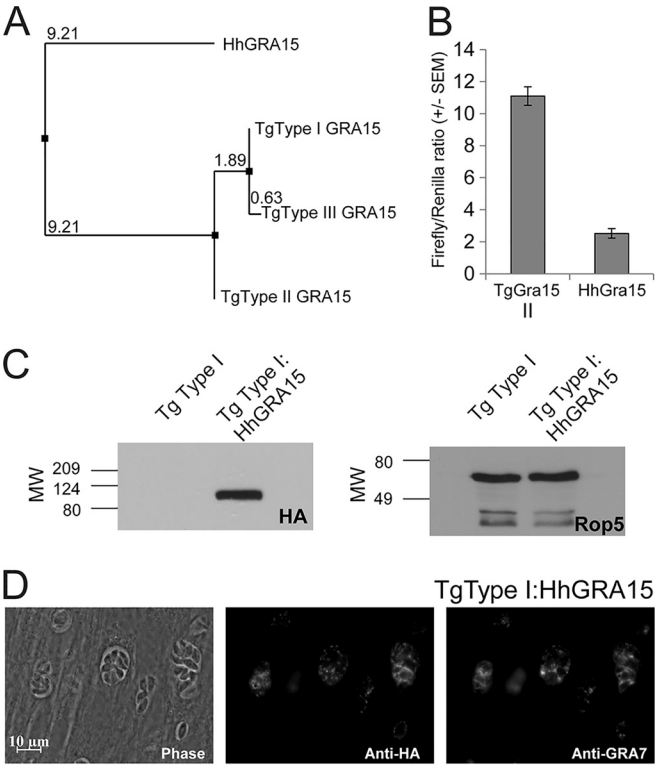

FIG 1 (A) Neighbor-joining tree based on percent identity between the published sequences for GRA15 from *T. gondii* types I, II, and III (GT1, ME49, and VEG, respectively) and that sequenced from *H. hammondi* HhGer041. (B) Dual-luciferase promoter assay comparing the efficacies of the putative promoters for $TgGRA15_{II}$ and HhGRA15. Data for two trials are shown as the ratios of firefly luciferase signal to *T. gondii* tubulin promoter-driven *Renilla* luciferase signal. (C) Western blot showing HA-tagged GRA15 (left) and loading control (ROP5). MW, molecular weight, in thousands. (D) Immunofluorescence assay showing colocalization of HA-tagged HhGRA15 with TgGRA7 in *T. gondii* strain RH.

***H. hammondi* ROP16 can increase STAT6 activation when expressed in *T. gondii*.** We identified a clear *H. hammondi* ortholog of *T. gondii* rhoptry protein 16 (ROP16) in our published *H. hammondi* genomic assembly and used these data to clone *HhROP16*. When we compared the putative promoter sequences of *HhROP16* and $TgROP16_{II}$, we identified a 16-bp deletion immediately preceding the predicted $TgROP16_{I,II,III}$ transcriptional start site (Fig. 3C; see also Fig. S3 in the supplemental material). When we fused the *HhROP16* upstream region to luciferase (as for GRA15 above) and compared its activity to that of the $TgROP16_{II}$ promoter in a type II strain, we found that the region 865 bp upstream of the *HhROP16* start codon was 25-fold less effective at driving luciferase expression than $TgROP16_{II}$ (Fig. 3B), and the *HhROP16* upstream sequence drove luciferase expression that was only 210-fold above background levels (see Table S1). This was in contrast to that observed for the *HhGRA15* promoter (above), which had activity that was ~6,000-fold higher than the background. When we deleted the 16 bp from the $TgROP16_{II}$ promoter, this significantly ($P = 0.002$) reduced promoter activity compared to that of TgROP16WT. When we inserted 16 bp from the TgROP16 promoter into the HhROP16 promoter, promoter activity increased but was not significantly different from that of the *H. hammondi* WT promoter ($P = 0.1$). This suggests that the

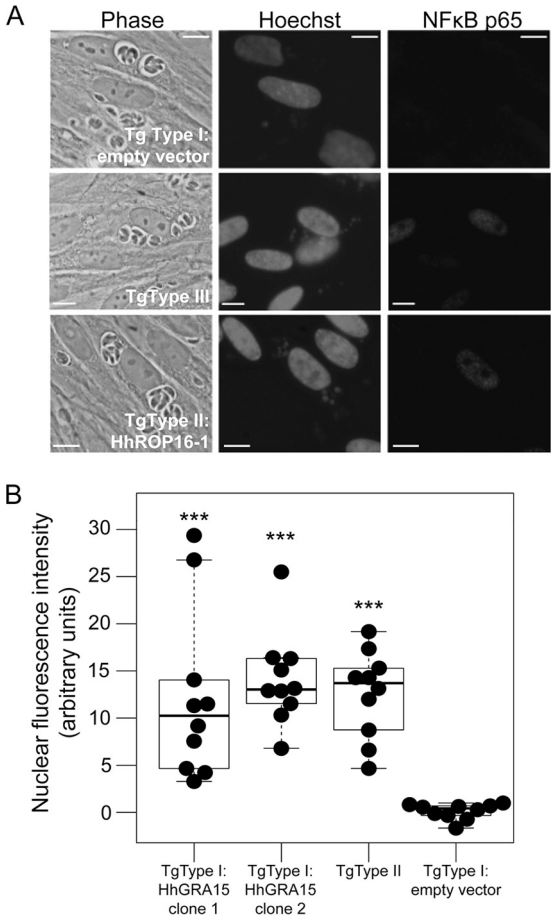

FIG 2 (A) Immunofluorescence analysis of NF-κB p65 activation. Infection (multiplicity of infection = 5) proceeded for 18 h before cells were fixed and stained for NF-κB p65. Like the *T. gondii* type II strain, *T. gondii* type I:HhGRA15 increases NF-κB translocation to the host cell nucleus. Scale bars: 10 μm. (B) *H. hammondi* HhGer041 GRA15 significantly increases the translocation of NF-κB. The mean fluorescent signal was quantified for 10 randomly chosen infected cells per strain. *T. gondii* type I-induced levels of NF-κB p65 were indistinguishable from the background, while levels in cells infected with *T. gondii* type II and *T. gondii* type I:HhGRA15 were similar ($P > 0.05$). ***, $P < 0.0001$ compared to *T. gondii* type I:empty vector.

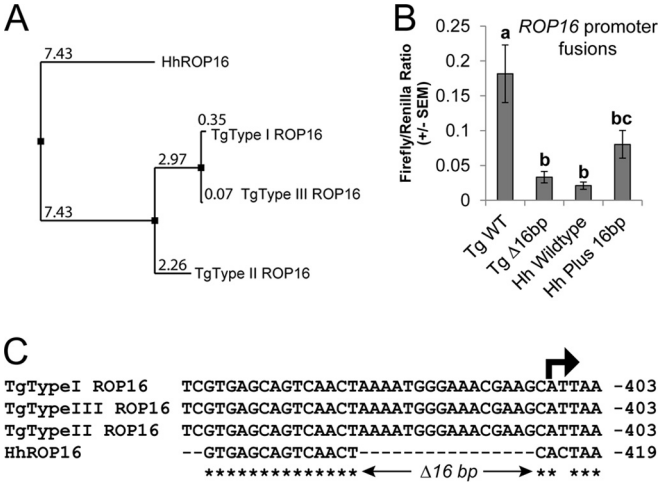

FIG 3 (A) Neighbor-joining tree based on percent identity between the published sequences for ROP16 from *T. gondii* types I, II, and III (GT1, ME49, and VEG, respectively) and that sequenced from *H. hammondi* HhGer041. (B) Dual-luciferase promoter assay comparing the efficacies of the putative promoters for $TgROP16_{II}$ WT and HhROP16 WT, as well as $TgROP16_{II}$ with a 16-bp deletion (Tg Δ16bp) and HhROP16 plus the 16 bp from the *Toxoplasma* promoters (Hh Plus 16bp). Data for 3 trials are shown as the ratios of firefly luciferase signal to *T. gondii* tubulin promoter-driven *Renilla* luciferase signal. Signal for the HhROP16 WT promoter was just slightly above the background. Means with the same letter are not significantly different ($P > 0.05$). (C) Alignment of the upstream region of the *ROP16* gene in *T. gondii* types I, II, and III and *H. hammondi* near the predicted transcriptional start site (arrow). Asterisks indicate nucleotides that are conserved across all four sequences.

HhROP16 promoter is ineffective compared to the syntenic sequence in *T. gondii* type II, and this difference is due, at least in part, to the deletion of 16 bp relative to the *T. gondii* promoter 1 bp upstream of the putative transcriptional start site (Fig. 3C).

The predicted HhROP16 protein is most similar to the *T. gondii* type II sequence (Fig. 3A), having the same amino acid at 20 of 38 sites encoding polymorphisms that distinguish $TgROP16_{II}$ from $TgROP16_{I/III}$ (see Fig. S4 in the supplemental material). In *T. gondii*, ROP16 is an active kinase that directly phosphorylates both STAT3 and STAT6, resulting in their translocation to the host cell nucleus (25, 53, 54). Strain types I and III are known to more strongly activate STAT3/6 translocation than type II strains, particularly after 18 h of infection (25). The difference in this ability between these strains is driven by a polymorphism in ROP16 at residue 503 (which is a leucine in *T. gondii* types I and III and a serine in *T. gondii* type II [54]), and HhROP16 shares the leucine residue with *T. gondii* clonotypes I and III (see Fig. S4).

Because the *H. hammondi ROP16* promoter drove weak luciferase expression, we expressed HhROP16 and $TgROP16_{II}$ in a type II strain of *T. gondii* using the constitutive *TgGRA1* promoter (55). Importantly, *GRA1* promoter-driven HhROP16 trafficked to the *T. gondii* rhoptry proteins as expected (Fig. 4A). We also examined whether, as has been shown for *T. gondii* ROP16 (25), *H. hammondi* ROP16 traffics to the host cell nucleus after infection. An important difference in the *H. hammondi* sequence is a single polymorphism in the putative nuclear localization signal (NLS) which meets the criteria for a monopartite class 4 NLS (Fig. 5D; see also Fig. S4 in the supplemental material) (56). To compare nuclear localizations of TgROP16 and HhROP16, we quantified the nuclear HA signal in host cells infected with either *T. gondii* type IΔ*ROP16*:$ROP16_{I\text{-}HA}$ (53) or *T. gondii* type II:$HhROP16_{HA}$. As expected, we found that all cells infected with parasites expressing an HA-tagged version of $TgROP16_{I}$ had visible nuclear HA staining, while this was the case in only ~40% of cells infected with parasites expressing $HhROP16_{HA}$ (Fig. 5A to C). The NLS in *T. gondii* ROP16 (RKRKRKQ) is required for trafficking into the host cell nucleus (25), although this trafficking is not required for activation of STAT3/6 (25). The ROP16 NLS is a class 4 NLS with the consensus sequence (R/P)XXK(R/K)(^DE), where ^DE indicates that the terminal residue in the motif cannot be an aspartic or glutamic acid residue (25, 56). Kosugi et al. showed that when the lysine in position 4 is changed to an arginine in this motif (the putative NLS of HhROP16 has an arginine at this residue [Fig. 5D]), it reduces the efficiency of, but does not eliminate, nuclear localization of a model protein in multiple cell types (56). Our data for HhROP16 were consistent with this observation.

When expressed in a *T. gondii* type II strain, GRA1 promoter-driven HhROP16 significantly increased STAT6 nuclear translo-

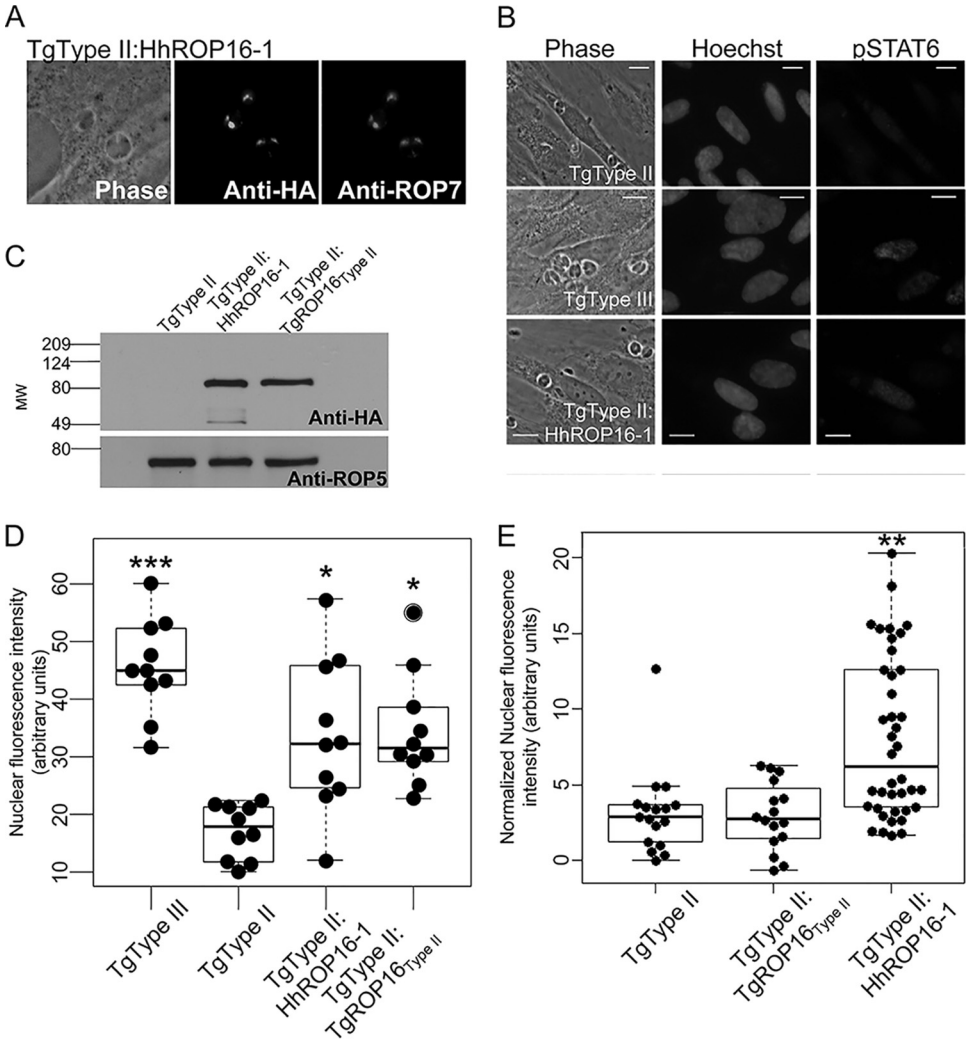

FIG 4 (A) Immunofluorescence of HA-tagged HhROP16 (driven by the *T. gondii* GRA1 promoter) showing colocalization with the rhoptry protein ROP7. (B) Immunofluorescence analysis of pSTAT6 signaling. Infection (multiplicity of infection = 5) proceeded for 24 h before cells were fixed and stained for pSTAT6. Similar to the *T. gondii* type III strain, *T. gondii* type II:HhROP16 increases translocation of phosphorylated STAT to the host cell nucleus. (C) Western blot showing expression of HA-tagged TgROP16 and HhROP16 in *T. gondii* type II and the ROP5 loading control. (D) *H. hammondi* ROP16 significantly increases pSTAT6 signaling in *T. gondii* type II. Nuclear fluorescence intensity was quantified for 10 randomly selected infected cells per strain. Cells infected with type II:HhROP16 have twice the pSTAT6 signal in their nuclei as cells infected with wild-type type II. Type III induces a greater translocation of pSTAT6 to the host cell nucleus than all other strains. *, $P < 0.05$, and ***, $P < 0.0001$, compared to signal in *T. gondii* type II. (E) *H. hammondi* ROP16 significantly increases pSTAT6 nuclear localization compared to *T. gondii* type II and type II expressing a second copy of $ROP16_{II}$. Cytoplasmic fluorescent signal was subtracted from nuclear fluorescent signal for ≥16 randomly chosen infected cells for each strain. **, $P < 0.001$ compared to *T. gondii* type II.

cation compared to that of the parental type II strain (Fig. 4B and D). Additionally, we expressed the type II allele of ROP16 in type II *T. gondii* using the same plasmid backbone (and GRA1 promoter), and Western blotting showed similar expression levels of HA-tagged ROP16 in both *T. gondii* type II:HhROP16 and *T. gondii* type II:$TgROP16_{II}$ parasites (Fig. 5C). While *T. gondii* type II:HhROP16 significantly increased nuclear pSTAT6 compared to *T. gondii* type II ($P < 0.001$), *T. gondii* type II:$TgROP16_{II}$ infection did not significantly alter pSTAT6 localization (Fig. 4E). Therefore, expressing an additional copy of $TgROP16_{II}$ is not sufficient to significantly increase pSTAT6 nuclear localization, indicating that the ability of HhROP16 to increase pSTAT6 activation during infection with type II *T. gondii* is likely due to differences in primary amino acid sequence (including leucine 503). With respect to the lower efficiency of nuclear localization of HhROP16 than for $TgROP16_{I}$, these data are consistent with what is known for TgROP16 (25): that nuclear trafficking of TgROP16 is not required for STAT6 activation and nuclear translocation. Regardless, the coding sequence of HhROP16 appears to be functionally conserved in terms of its ability to increase STAT6 activation, at least when driven by a constitutive promoter in a *T. gondii* type II strain, and based on its higher efficacy than for $TgROP16_{II}$, it is likely most similar in function to the type I and type III ROP16 alleles.

The transcriptional profiles of *H. hammondi* HhCatGER041 and *T. gondii* VEG sporulated oocysts are distinct. We compared transcriptional profiles of *H. hammondi* (HhCatGer041) and *T. gondii* (VEG) sporulated oocysts using *T. gondii* Affymetrix

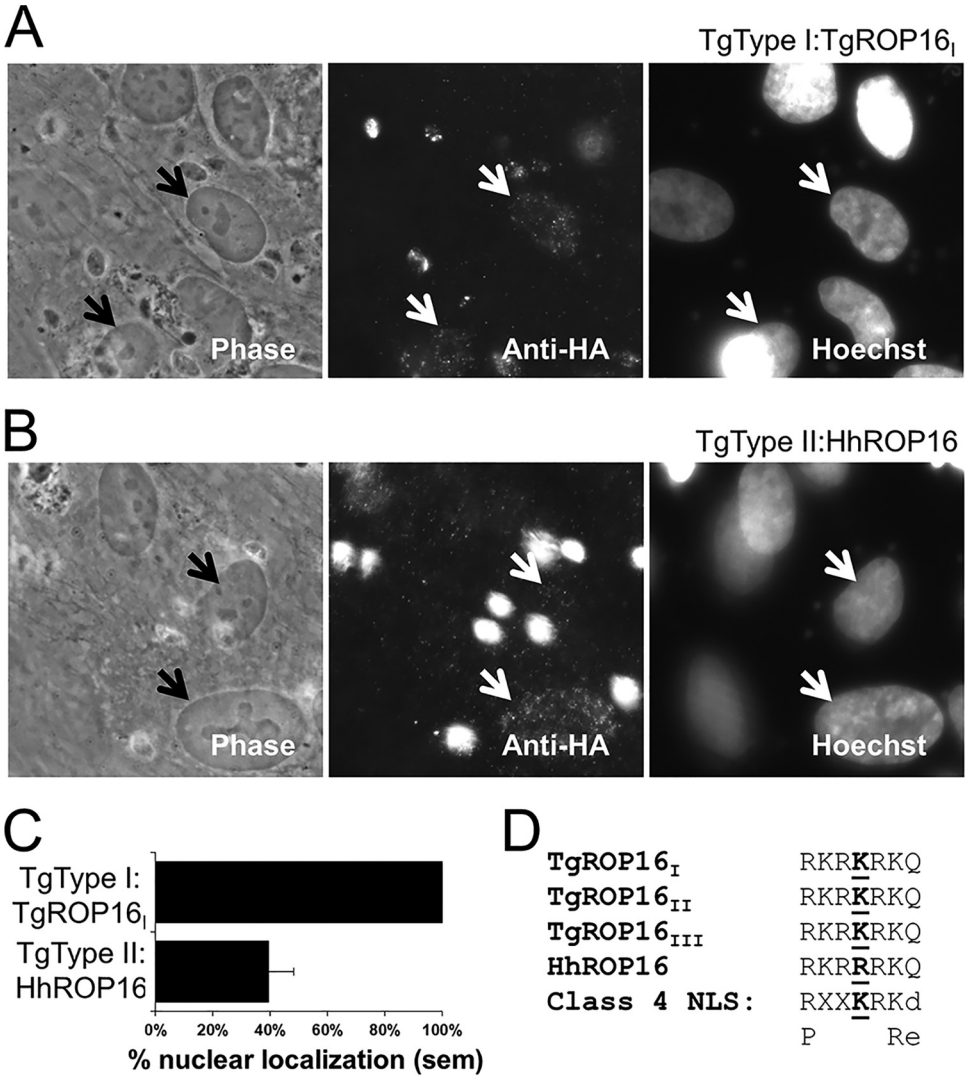

FIG 5 (A) Nuclear localization of TgROP16$_I$ in cells infected with *T. gondii* type IΔROP16:TgROP16$_I$ 18 h postinfection. Arrows indicate two infected cells that show significant nuclear HA signal. (B) Inconsistent nuclear localization of HhROP16 in cells infected with *T. gondii* type II:HhROP16 18 h postinfection. Arrows indicate two infected cells, one with minimal nuclear anti-HA staining (top arrow) and another with clear nuclear anti-HA staining (bottom arrow). (C) Quantification of the percentage of infected cells exhibiting visible nuclear HA staining when infected with either *T. gondii* type IΔROP16:TgROP16$_I$ or *T. gondii* type II:HhROP16. Data shown from 20 infected cells. sem, standard error of the mean. (D) Alignment of the nuclear localization signal (NLS) in *T. gondii* type I, II, and III ROP16 and *H. hammondi* ROP16 (top 4 sequences) showing the residue at position 4 that is uniquely changed to arginine in *H. hammondi* ROP16. The fifth sequence is the consensus sequence for a type 4 NLS, and the last sequence shows alternative amino acids. Uppercase letters indicate permitted amino acids, and lowercase letters indicate nonpermissible amino acids.

expression arrays (37). We used sporulated oocysts due to the difficulties in long-term *in vitro* culture of *H. hammondi* tachyzoites (9, 16). The transcriptional profiles of these species were comparable but had some striking differences (Fig. 6). Using statistical analyses, we identified 78 genes of significantly greater abundance in *H. hammondi* ("Hh-high" [see Fig. S5 in the supplemental material]) and 80 significantly higher in *T. gondii* strain VEG ("Tg-high" [see Fig. S6 in the supplemental material]). Gene ontology (GO) analysis of these gene sets did not identify any enriched GO terms in the Hh-high gene set, although 4 significant GO categories were enriched in the Tg-high set: GO:0003735 (structural constituent of ribosome; $P = 2.60E{-}08$), GO:0006412 (translation; $P = 2.91E{-}08$), GO:0005840 (ribosome; $P = 1.40E{-}07$), and GO:0015935 (small ribosomal subunit; $P = 0.019$). The genes in these categories coded for both large and small ribosomal subunits (see Table S2 in the supplemental material) and were 10- to 42-fold more abundant in *T. gondii* sporulated oocysts than in *H. hammondi*. In addition to GO categories, we also analyzed all other currently available ToxoDB gene annotations using GeneMerge. We found that the Tg-high and Hh-high sets were not significantly enriched for genes in any particular annotation except the GO categories listed above, including the presence or absence of a putative signal peptide.

We also compared these transcript data to the previously published transcriptional profile from multiple life stages of *T. gondii* type II strain M4 (including unsporulated and sporulated oocysts, tachyzoites, and *in vitro* and *in vivo* bradyzoite cysts [39, 40]). Overall, the majority of the Tg-high set were expressed not only in

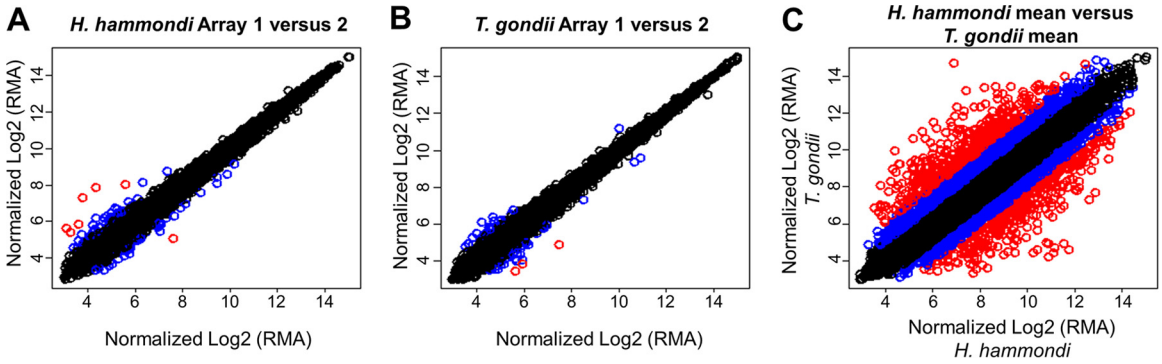

FIG 6 Plots of normalized, $\log_2$-transformed hybridization intensities within (A and B) and between (C) species. The plots in panels A and B are derived from replicate arrays within each species, and the plot in panel C is the mean across the 3 arrays for each species. The intensities for each gene are color-coded based on the absolute values of the fold difference in transcript abundance as follows: black, ≤2-fold; blue, between 2- and 4-fold; red, ≥4-fold. RMA, robust multiarray average.

T. gondii oocyst/sporozoite stages but also in other M4 life stages. This was in contrast to the Hh-high gene set, and by comparing these data to the M4 data set, we identified two distinct clusters for further analysis: one where Hh-high transcripts were low in all *T. gondii* VEG and M4 life stages analyzed ("Hh-specific") and another where Hh-high transcripts were high in *T. gondii* cyst stages ("Hh-TgCyst-high"; see Fig. S5). In support of the existence of an Hh-TgCyst-high set was a significant ($P = 0.0011$) overlap between the Hh-high gene set and an empirically determined gene set that is upregulated during the transition from tachyzoites to bradyzoites *in vivo* and/or *in vitro* in *T. gondii* strain M4. To identify these genes in an unbiased way, we used Pavlidis template matching (47) at an adjusted *P* value threshold of 1×10^{-6} and identified 9 Hh-TgCyst-high genes and 38 Hh-specific genes (Fig. 7A and B, respectively) that significantly matched the respective templates. GO analysis on both gene sets did not identify any significant GO category enrichment. However, included in the Hh-specific set was a predicted AP2 transcription factor, APVIIB2. Transcript abundance for this gene was low in *T. gondii* VEG sporulated oocysts and all M4 life cycle stages (Fig. 7B). While this was the only AP2 transcription factor family member that was of significantly higher abundance in *H. hammondi* than in *T. gondii*, among the 53 AP2 family members analyzed on the microarray, *APIX8* and *APVIII5* transcript levels were also 6-fold higher in *H. hammondi* than in *T. gondii* VEG sporulated oocysts (see Fig. S9 in the supplemental material), and these transcripts are upregulated during the tachyzoite-to-bradyzoite transition in *T. gondii* strain M4 (arrowheads in Fig. S9). Genes in the Hh-TgCyst-high set included genes for a bradyzoite-specific NTPase and multiple hypothetical proteins (Fig. 7B). In contrast to these major differences in transcription between *T. gondii* and *H. hammondi*, we detected no significant expression differences between *H. hammondi* and *T. gondii* VEG sporulated oocyst transcript levels for *T. gondii* secreted effectors like ROP5, ROP18, ROP16, and GRA15 (Fig. 7C). Overall, these data show that *H. hammondi* sporulated oocysts have a unique expression profile compared to that of *T. gondii* sporulated oocysts, and some of these differentially regulated genes are highly expressed in *T. gondii* M4 bradyzoites.

DISCUSSION

Our recently published genome sequence of an isolate of *H. hammondi* (HhCatGer041 [28]; GenBank accession number AVCM00000000.1) revealed a high degree of genomic synteny and conservation with *T. gondii*, further confirming *H. hammondi* as the closest known extant relative of *T. gondii* (28). Despite this high sequence similarity, there are dramatic phenotypic differences between *H. hammondi* and *T. gondii*. Unlike *T. gondii*, *H. hammondi* spontaneously converts to slow-growing tissue cyst stages *in vitro* and cannot be propagated indefinitely *in vitro* (9, 16). This has also been shown *in vitro* for another *Hammondia* sp. isolated from foxes (57), now named *H. triffittae* (58). *H. hammondi* is relatively avirulent in mice (including interferon gamma knockouts [9, 16]) and has never been shown to cause disease in humans. The genetics underlying these phenotypic differences are unknown. They could be due to differences in gene content due to gene gain and loss during and after divergence of these species. The also could be due to distinct transcriptional profiles. Building off previous work showing that *H. hammondi* orthologs of the *T. gondii* virulence effectors ROP18 and ROP5 are functionally conserved when expressed in *T. gondii* (28), in the present study we examined the efficacy of the syntenic *H. hammondi* orthologs of GRA15 (27) and ROP16 (25). Our assay for functional conservation was 2-fold: (i) was the *H. hammondi* ortholog effectively expressed in *T. gondii*, and (ii) could the *H. hammondi* ortholog complement a known cell signaling phenotype?

The *H. hammondi GRA15* promoter was functional when expressed heterologously in *T. gondii*, while the *H. hammondi ROP16* promoter was far less effective (see Table S1 in the supplemental material). The promoters for *H. hammondi ROP16* and *T. gondii ROP16* are highly conserved, but there is a16-bp deletion just upstream of the putative transcriptional start site in the *H. hammondi ROP16* promoter. No such differences exist in the *H. hammondi* and *T. gondii GRA15* upstream sequences. The deletion in the HhROP16 promoter is similar to previous observations for the *H. hammondi* and *T. gondii ROP18* promoters. In the *ROP18* gene there is a 107-bp sequence present in *T. gondii* strains that actively express ROP18 (such as strain types I and II [15, 23]) as well as *HhROP18* (28) but absent in *T. gondii* strains that do not express ROP18 (such as members of the type III lineage [15, 23]). The *HhROP18* promoter is fully active in luciferase reporter assays and drives HhROP18 protein expression in *T. gondii*, and this dramatically alters virulence; this 107-bp sequence is both necessary and sufficient for *ROP18* promoter-driven reporter expression (28). In the present study, we found that the 16 bp deleted in

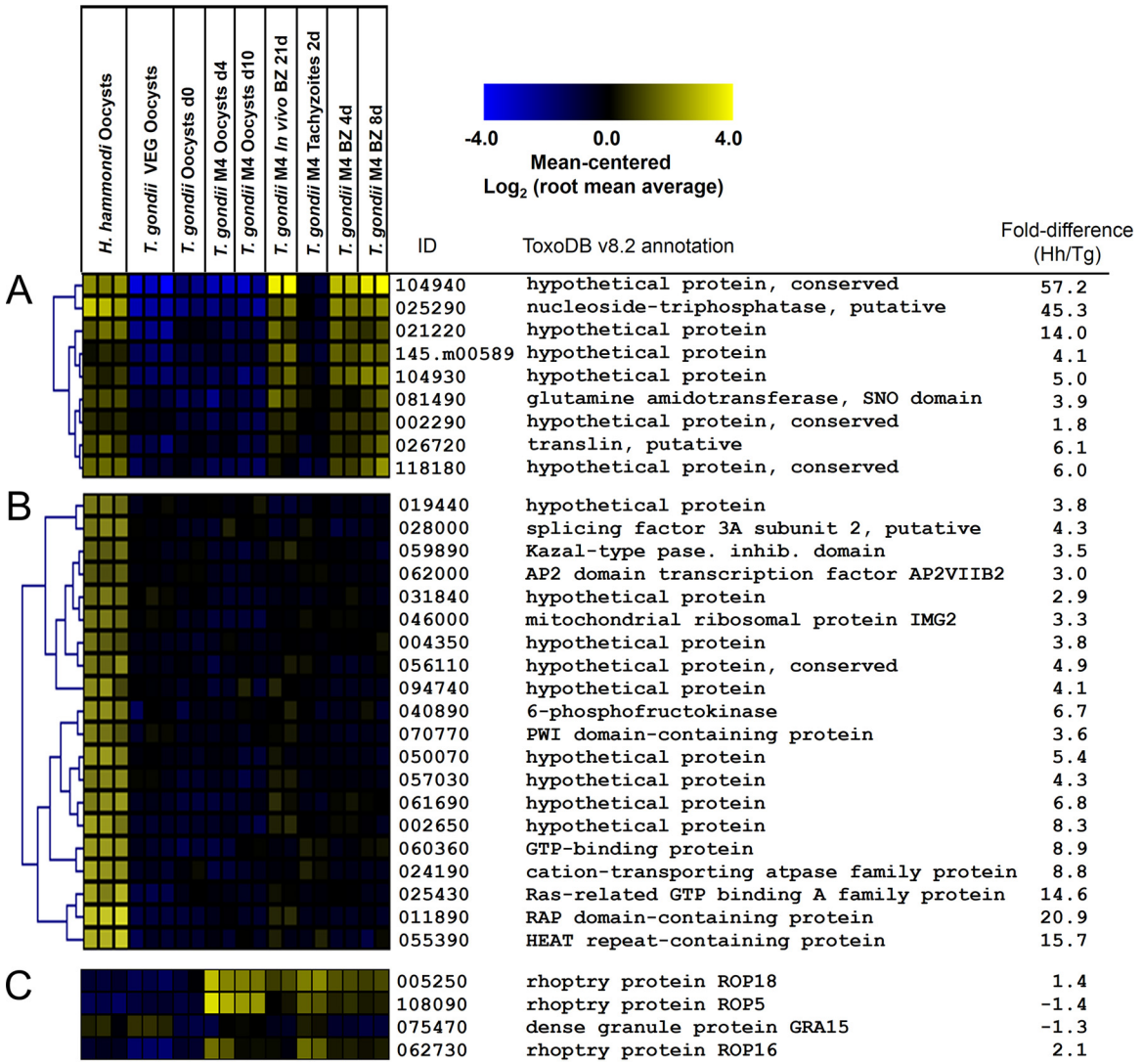

FIG 7 Transcript abundance in *H. hammondi* HhCatGer041 and *T. gondii* VEG sporozoites for 9 genes of higher transcript abundance in *H. hammondi* sporozoites as well as *T. gondii* cyst stages (Hh-TgCyst-high) (A), a subset of genes of high abundance in *H. hammondi* sporozoites that were of low abundance in *T. gondii* VEG and all M4 life cycle stages (B), and known *T. gondii* effectors (rhoptry proteins ROP5, ROP16, and ROP18 and dense granule protein GRA15). Data from a previously published data set profiling the transcriptome of multiple life cycle stages of *T. gondii* strain M4 (GEO series GSE32427) are shown for comparison, and gene identifications are based on ME49B7 annotation version 7.2.

the *HhROP16* promoter play an important role in the ability of the *ROP16* upstream sequence to drive reporter gene expression, suggesting that this is an important core promoter sequence for *ROP16*. This result further confirms the utility of comparative genomic analysis to identify regulatory regions that are important for the expression of *T. gondii* effector proteins like ROP18 and ROP16. It is important to note that the lack of activity of the *H. hammondi ROP16* promoter when expressed in *T. gondii* does not prove that the *H. hammondi ROP16* gene is not expressed in its native context (i.e., within *H. hammondi* itself). At least in sporulated oocysts there were no differences in *ROP16* transcript abundance between *H. hammondi* and *T. gondii* VEG sporozoites, although the *ROP16* transcript was detectable in both species. Transcriptome analyses of *H. hammondi* tachyzoites will be necessary to determine if this difference in promoter function in a heterologous expression system is recapitulated *in vivo*. While such experiments are significantly hampered by the inability to grow *H. hammondi* indefinitely *in vitro*, deep RNA sequencing technology will be useful to circumvent this problem.

When expressed in a type I strain of *T. gondii*, *H. hammondi* GRA15 leads to significantly more NF-κB p65 activation than a wild-type type I strain. It has been shown that the type II allele of *T. gondii* GRA15 is a much more potent activator of NF-κB signaling than the alleles from *T. gondii* clonotypes I and III (27). *H. hammondi* GRA15 can increase NF-κB p65 activation in a *T. gondii* type I strain to levels that are very similar to that of a wild-type *T. gondii* type II strain (Fig. 2B), suggesting that *H. hammondi* GRA15 behaves like a *T. gondii* type II GRA15 allele. Our sequence analysis shows that while overall HhGRA15 is most similar to *T. gondii* GRA15 alleles from types I and III, this is quantitatively driven by the fact that HhGRA15 shares an 84-amino-acid sequence with $TgGRA15_{I/III}$ that is deleted in $TgGRA15_{II}$. These data

indicate that the sequence in HhGRA15 and Tg*GRA15*$_{I/III}$ relative to Tg*GRA15*$_{II}$ is ancestral to the *T. gondii* lineage (and therefore is likely to be a deletion in TgGRA15$_{II}$). Moreover, the fact that expressing HhGRA15 in *T. gondii* type I increases its ability to activate NF-κB to levels that are similar to those in type II strains indicates that the C-terminal deletion in TgGRA15$_{II}$ is not responsible for differences in the ability of *T. gondii* alleles to activate NF-κB, a possibility proposed by Rosowski et al. (27). Further experiments, such as complementing a type I strain with a type I GRA15 allele and comparing its efficacy to those of HhGRA15 and TgGRA15$_{II}$, will be necessary to determine whether HhGRA15 behaves identically to TgGRA15$_{II}$. If it does, this would implicate only 3 polymorphisms present in both TgGRA15$_{II}$ and HhGRA15 as being potentially responsible for the significant phenotypic differences between TgGRA15$_{II}$ and TgGRA15$_{I/III}$.

When expressed off a highly active promoter in *T. gondii*, HhROP16 is less efficient at trafficking to the host cell nucleus than TgROP16$_{I}$, but it still increases STAT6 nuclear translocation when expressed in a *T. gondii* type II strain. At the amino acid level, *H. hammondi* ROP16 is most similar to *T. gondii* type II ROP16, and therefore, the increase in STAT6 activation shown in Fig. 4D could be due to gene dosage effects (*T. gondii* type II:*HhROP16* also has an endogenous copy of *TgROP16*) rather than HhROP16 being more functionally similar to TgROP16$_{I/III}$. To test this, we created a type II *T. gondii* parasite clone with an additional copy of ROP16$_{II}$ (driven by the same TgGRA1 promoter as HhROP16) and compared STAT6 activation driven by this strain to those in wild-type type II *T. gondii* and type II *T. gondii* expressing HhROP16. We found that *T. gondii* type II:TgROP16$_{II}$ was no more capable of STAT6 activation than *T. gondii* type II:WT, while again *T. gondii* type II:HhROP16 significantly activated STAT6 (Fig. 4E). These data further support a major role for residue 503 in HhROP16 and TgROP16$_{I/III}$, which is a serine in both HhROP16 and TgROP16I/III and has been shown to be required for the phosphorylation of STAT3 by TgROP16$_{I/III}$ (and which is a serine in TgROP16$_{II}$ which does not phosphorylate STAT3 [25, 54]).

As mentioned above, these data do not address whether the promoters for *H. hammondi* ROP16 and GRA15 are actually functional in their native context within *H. hammondi* during acute infection. Such an analysis is hampered by the fact that *H. hammondi* sporozoites spontaneously convert to bradyzoite cysts *in vitro* and to date cannot be subcultured (5, 9, 16, 59). This is in contrast even to *T. gondii* VEG strain sporozoites, which, although they also form bradyzoite cysts spontaneously *in vitro* (60), can be subcultured and eventually grow as rapidly growing tachyzoites (60).

The transcriptional data in the present study are from sporozoites isolated from *T. gondii* and *H. hammondi* oocysts and represent the first transcriptional comparison between these species. These data show that the sporulated oocyst transcriptomes for these species are highly distinct. Among the genes of greater abundance in *H. hammondi* than in *T. gondii* VEG, a subset were highly expressed only in *H. hammondi* sporozoites compared to both *T. gondii* VEG and M4 sporozoites and multiple M4 life cycle stages. These "Hh-specific" genes are interesting candidates that may underlie phenotypic differences between these species. Of particular interest in the Hh-specific gene set was the AP2 transcription factor AP2VIIB2 (Fig. 7B), which not only is of low abundance in the M4 data set but also is consistently of low abundance (<40th percentile) in 15 microarray and transcriptome sequencing expression data sets from multiple strains and life stages available for this gene on ToxoDB (v8.2 gene name, TGME49_262000). Given emerging discoveries regarding the importance of the AP2 transcription factor family in *T. gondii* developmental processes, particularly those involving tachyzoite-to-bradyzoite conversion (61–63)), this is a particularly intriguing candidate gene for mediating transcriptional differences between these species, at least in sporulated oocysts.

Another subset of Hh-high transcripts are developmentally regulated during the tachyzoite-to-bradyzoite transition in *T. gondii* strain M4 (both *in vitro* and *in vivo*). Two other AP2 family members were over 6-fold more abundant in *H. hammondi* sporulated oocysts than in *T. gondii*, and while these were not significantly different, they do appear to also be upregulated in strain M4 bradyzoites (both *in vivo* and *in vitro*). In addition, multiple members of the Hh-high gene set are at least slightly upregulated in M4 bradyzoites compared to tachyzoites. This observation, coupled with their significantly higher expression in *H. hammondi* sporulated oocysts than in *T. gondii* VEG, fits with the dramatic growth differences between these species both *in vitro* and *in vivo*. The expression patterns of "bradyzoite" genes in *H. hammondi* sporulated oocysts may be a reflection of their place on the developmental spectrum between tachyzoite and bradyzoite. This spectrum has been described previously for *T. gondii* strains that differ in their growth characteristics *in vitro* (e.g., VEG compared to RH [64]) but has yet to be described in multispecies comparisons like those outlined in the present study.

Transcriptional comparisons between *T. gondii* and *Neospora caninum*, a fellow coccidian that is more diverged from *T. gondii* than *H. hammondi*, have been reported (65). *N. caninum* tachyzoites have significantly lower ROP16 transcript levels than *T. gondii*, and it was proposed that despite the conserved leucine residue crucial for ROP16-driven STAT3 phosphorylation in *N. caninum* ROP16, this strain of *N. caninum* would be unlikely to modulate the STAT3 (or possibly STAT6) pathway (65). This has yet to be tested empirically, and attempts to align the upstream regions of NcROP16, HhROP16, and TgROP16 were not possible given the high divergence of the NcROP16 upstream sequence.

ACKNOWLEDGMENTS

We acknowledge John Boothroyd (Stanford University) for providing the ROP16$_{HA}$-complemented *T. gondii* strain and Eric Polinko (University of Pittsburgh) for computing support.

This work was supported by a Pew Scholarship in the Biomedical Sciences to J.P.B. and by University of Pittsburgh Biological Sciences summer and academic year fellowships funded by the Howard Hughes Medical Institute to K.A.W., R.A.D., A.L.B., and A.R.S.

We declare no conflict of interest.

REFERENCES

1. **Jones JL, Kruszon-Moran D, Wilson M, McQuillan G, Navin T, McAuley JB.** 2001. *Toxoplasma gondii* infection in the United States: seroprevalence and risk factors. Am. J. Epidemiol. **154:**357–365. http://dx.doi.org/10.1093/aje/154.4.357.
2. **Israelski DM, Remington JS.** 1993. Toxoplasmosis in patients with cancer. Clin. Infect. Dis. **17**(Suppl 2):S423–S435.
3. **Luft BJ, Hafner R, Korzun AH, Leport C, Antoniskis D, Bosler EM, Bourland DD, III, Uttamchandani R, Fuhrer J, Jacobson J, Morlat P, Vilde J-L, Remington JS,** ACTG 077p/ANRS 009 Study Team. 1993. Toxoplasmic encephalitis in patients with the acquired immunodeficiency syndrome. N. Engl. J. Med. **329:**995–1000.

4. **Remington JS, Klein JO.** 2001. Infectious diseases of the fetus and newborn infant, 5th ed. Saunders, Philadelphia, PA.
5. **Frenkel JK, Dubey JP.** 1975. *Hammondia hammondi* gen. nov., sp. nov., from domestic cats, a new coccidian related to *Toxoplasma* and *Sarcocystis*. Z. Parasitenkd. **46:**3–12. http://dx.doi.org/10.1007/BF00383662.
6. **Carme B, Demar M, Ajzenberg D, Darde ML.** 2009. Severe acquired toxoplasmosis caused by wild cycle of *Toxoplasma gondii*, French Guiana. Emerg. Infect. Dis. **15:**656–658. http://dx.doi.org/10.3201/eid1504.081306.
7. **Dubey JP.** 1998. Advances in the life cycle of *Toxoplasma gondii*. Int. J. Parasitol. **28:**1019–1024. http://dx.doi.org/10.1016/S0020-7519(98)00023-X.
8. **Wong SY, Remington JS.** 1993. Biology of *Toxoplasma gondii*. AIDS **7:**299–316.
9. **Dubey JP, Sreekumar C.** 2003. Redescription of *Hammondia hammondi* and its differentiation from *Toxoplasma gondii*. Int. J. Parasitol. **33:**1437–1453. http://dx.doi.org/10.1016/S0020-7519(03)00141-3.
10. **Mugridge NB, Morrison DA, Heckeroth AR, Johnson AM, Tenter AM.** 1999. Phylogenetic analysis based on full-length large subunit ribosomal RNA gene sequence comparison reveals that *Neospora caninum* is more closely related to *Hammondia heydorni* than to *Toxoplasma gondii*. Int. J. Parasitol. **29:**1545–1556. http://dx.doi.org/10.1016/S0020-7519(99)00150-2.
11. **Su C, Evans D, Cole RH, Kissinger JC, Ajioka JW, Sibley LD.** 2003. Recent expansion of *Toxoplasma* through enhanced oral transmission. Science **299:**414–416. http://dx.doi.org/10.1126/science.1078035.
12. **Su C, Khan A, Zhou P, Majumdar D, Ajzenberg D, Darde ML, Zhu XQ, Ajioka JW, Rosenthal BM, Dubey JP, Sibley LD.** 2012. Globally diverse *Toxoplasma gondii* isolates comprise six major clades originating from a small number of distinct ancestral lineages. Proc. Natl. Acad. Sci. U. S. A. **109:**5844–5849. http://dx.doi.org/10.1073/pnas.1203190109.
13. **Khan A, Miller N, Roos DS, Dubey JP, Ajzenberg D, Darde ML, Ajioka JW, Rosenthal B, Sibley LD.** 2011. A monomorphic haplotype of chromosome Ia is associated with widespread success in clonal and nonclonal populations of *Toxoplasma gondii*. mBio **2**(6):e00228–11. http://dx.doi.org/10.1128/mBio.00228-11.
14. **Boyle JP, Saeij JP, Boothroyd JC.** 2007. *Toxoplasma gondii*: inconsistent dissemination patterns following oral infection in mice. Exp. Parasitol. **116:**302–305. http://dx.doi.org/10.1016/j.exppara.2007.01.010.
15. **Saeij JP, Boyle JP, Coller S, Taylor S, Sibley LD, Brooke-Powell ET, Ajioka JW, Boothroyd JC.** 2006. Polymorphic secreted kinases are key virulence factors in toxoplasmosis. Science **314:**1780–1783. http://dx.doi.org/10.1126/science.1133690.
16. **Dubey JP, Tilahun G, Boyle JP, Schares G, Verma SK, Ferreira LR, Oliveira S, Tiao N, Darrington C, Gebreyes WA.** 2013. Molecular and biological characterization of first isolates of *Hammondia hammondi* from cats from Ethiopia. J. Parasitol. **99:**614–618. http://dx.doi.org/10.1645/12-51.1.
17. **Araujo FG, Dubey JP, Remington JS.** 1984. Antigenic similarity between the coccidian parasites *Toxoplasma gondii* and *Hammondia hammondi*. J. Protozool. **31:**145–147. http://dx.doi.org/10.1111/j.1550-7408.1984.tb04304.x.
18. **Behnke MS, Khan A, Wootton JC, Dubey JP, Tang K, Sibley LD.** 2011. Virulence differences in *Toxoplasma* mediated by amplification of a family of polymorphic pseudokinases. Proc. Natl. Acad. Sci. U. S. A. **108:**9631–9636. http://dx.doi.org/10.1073/pnas.1015338108.
19. **Fleckenstein MC, Reese ML, Konen-Waisman S, Boothroyd JC, Howard JC, Steinfeldt T.** 2012. A *Toxoplasma gondii* pseudokinase inhibits host IRG resistance proteins. PLoS Biol. **10:**e1001358. http://dx.doi.org/10.1371/journal.pbio.1001358.
20. **Khaminets A, Hunn JP, Konen-Waisman S, Zhao YO, Preukschat D, Coers J, Boyle JP, Ong YC, Boothroyd JC, Reichmann G, Howard JC.** 2010. Coordinated loading of IRG resistance GTPases on to the *Toxoplasma gondii* parasitophorous vacuole. Cell. Microbiol. **12:**939–961. http://dx.doi.org/10.1111/j.1462-5822.2010.01443.x.
21. **Niedelman W, Gold DA, Rosowski EE, Sprokholt JK, Lim D, Farid Arenas A, Melo MB, Spooner E, Yaffe MB, Saeij JP.** 2012. The rhoptry proteins ROP18 and ROP5 mediate *Toxoplasma gondii* evasion of the murine, but not the human, interferon-gamma response. PLoS Pathog. **8:**e1002784. http://dx.doi.org/10.1371/journal.ppat.1002784.
22. **Reese ML, Zeiner GM, Saeij JP, Boothroyd JC, Boyle JP.** 2011. Polymorphic family of injected pseudokinases is paramount in *Toxoplasma* virulence. Proc. Natl. Acad. Sci. U. S. A. **108:**9625–9630. http://dx.doi.org/10.1073/pnas.1015980108.
23. **Taylor S, Barragan A, Su C, Fux B, Fentress SJ, Tang K, Beatty WL, Hajj HE, Jerome M, Behnke MS, White M, Wootton JC, Sibley LD.** 2006. A secreted serine-threonine kinase determines virulence in the eukaryotic pathogen *Toxoplasma gondii*. Science **314:**1776–1780. http://dx.doi.org/10.1126/science.1133643.
24. **Butcher BA, Fox BA, Rommereim LM, Kim SG, Maurer KJ, Yarovinsky F, Herbert DR, Bzik DJ, Denkers EY.** 2011. *Toxoplasma gondii* rhoptry kinase ROP16 activates STAT3 and STAT6 resulting in cytokine inhibition and arginase-1-dependent growth control. PLoS Pathog. **7:**e1002236. http://dx.doi.org/10.1371/journal.ppat.1002236.
25. **Saeij JP, Coller S, Boyle JP, Jerome ME, White MW, Boothroyd JC.** 2007. *Toxoplasma* co-opts host gene expression by injection of a polymorphic kinase homologue. Nature **445:**324–327. http://dx.doi.org/10.1038/nature05395.
26. **Jensen KD, Wang Y, Wojno ED, Shastri AJ, Hu K, Cornel L, Boedec E, Ong YC, Chien YH, Hunter CA, Boothroyd JC, Saeij JP.** 2011. *Toxoplasma* polymorphic effectors determine macrophage polarization and intestinal inflammation. Cell Host Microbe **9:**472–483. http://dx.doi.org/10.1016/j.chom.2011.04.015.
27. **Rosowski EE, Lu D, Julien L, Rodda L, Gaiser RA, Jensen KD, Saeij JP.** 2011. Strain-specific activation of the NF-kappaB pathway by GRA15, a novel *Toxoplasma gondii* dense granule protein. J. Exp. Med. **208:**195–212. http://dx.doi.org/10.1084/jem.20100717.
28. **Walzer KA, Adomako-Ankomah Y, Dam RA, Herrmann DC, Schares G, Dubey JP, Boyle JP.** 2013. *Hammondia hammondi*, an avirulent relative of *Toxoplasma gondii*, has functional orthologs of known *T. gondii* virulence genes. Proc. Natl. Acad. Sci. U. S. A. **110:**7446–7451. http://dx.doi.org/10.1073/pnas.1304322110.
29. **Wakaguri H, Suzuki Y, Katayama T, Kawashima S, Kibukawa E, Hiranuka K, Sasaki M, Sugano S, Watanabe J.** 2009. Full-Malaria/Parasites and Full-Arthropods: databases of full-length cDNAs of parasites and arthropods, update 2009. Nucleic Acids Res. **37:**D520–D525. http://dx.doi.org/10.1093/nar/gkn856.
30. **Trujillo M, Donald RG, Roos DS, Greene PJ, Santi DV.** 1996. Heterologous expression and characterization of the bifunctional dihydrofolate reductase-thymidylate synthase enzyme of *Toxoplasma gondii*. Biochemistry **35:**6366–6374. http://dx.doi.org/10.1021/bi952923q.
31. **Hartley JL, Temple GF, Brasch MA.** 2000. DNA cloning using *in vitro* site-specific recombination. Genome Res. **10:**1788–1795. http://dx.doi.org/10.1101/gr.143000.
32. **Boyle JP, Saeij JP, Harada SY, Ajioka JW, Boothroyd JC.** 2008. Expression quantitative trait locus mapping of *Toxoplasma* genes reveals multiple mechanisms for strain-specific differences in gene expression. Eukaryot. Cell **7:**1403–1414. http://dx.doi.org/10.1128/EC.00073-08.
33. **Gissot M, Kelly KA, Ajioka JW, Greally JM, Kim K.** 2007. Epigenomic modifications predict active promoters and gene structure in *Toxoplasma gondii*. PLoS Pathog. **3:**e77. http://dx.doi.org/10.1371/journal.ppat.0030077.
34. **Donald RG, Carter D, Ullman B, Roos DS.** 1996. Insertional tagging, cloning, and expression of the *Toxoplasma gondii* hypoxanthine-xanthine-guanine phosphoribosyltransferase gene. Use as a selectable marker for stable transformation. J. Biol. Chem. **271:**14010–14019.
35. **Parmley SF, Sgarlato GD, Remington JS.** 1993. Genomic and corrected cDNA sequence of the P28 gene from *Toxoplasma gondii*. Mol. Biochem. Parasitol. **57:**161–165. http://dx.doi.org/10.1016/0166-6851(93)90253-T.
36. **Rome ME, Beck JR, Turetzky JM, Webster P, Bradley PJ.** 2008. Intervacuolar transport and unique topology of GRA14, a novel dense granule protein in *Toxoplasma gondii*. Infect. Immun. **76:**4865–4875. http://dx.doi.org/10.1128/IAI.00782-08.
37. **Bahl A, Davis PH, Behnke M, Dzierszinski F, Jagalur M, Chen F, Shanmugam D, White MW, Kulp D, Roos DS.** 2010. A novel multifunctional oligonucleotide microarray for *Toxoplasma gondii*. BMC Genomics **11:**603. http://dx.doi.org/10.1186/1471-2164-11-603.
38. **Altschul SF, Madden TL, Schaffer AA, Zhang J, Zhang Z, Miller W, Lipman DJ.** 1997. Gapped BLAST and PSI-BLAST: a new generation of protein database search programs. Nucleic Acids Res. **25:**3389–3402. http://dx.doi.org/10.1093/nar/25.17.3389.
39. **Fritz HM, Buchholz KR, Chen X, Durbin-Johnson B, Rocke DM, Conrad PA, Boothroyd JC.** 2012. Transcriptomic analysis of *Toxoplasma* development reveals many novel functions and structures specific to sporozoites and oocysts. PLoS One **7:**e29998. http://dx.doi.org/10.1371/journal.pone.0029998.
40. **Buchholz KR, Fritz HM, Chen X, Durbin-Johnson B, Rocke DM, Ferguson DJ, Conrad PA, Boothroyd JC.** 2011. Identification of tissue

cyst wall components by transcriptome analysis of *in vivo* and *in vitro* *Toxoplasma gondii* bradyzoites. Eukaryot. Cell **10:**1637–1647. http://dx.doi.org/10.1128/EC.05182-11.
41. **R Development Core Team.** 2011. R: a language and environment for statistical computing. R Foundation for Statistical Computing, Vienna, Austria.
42. **Gautier L, Cope L, Bolstad BM, Irizarry RA.** 2004. affy—analysis of Affymetrix GeneChip data at the probe level. Bioinformatics **20:**307–315. http://dx.doi.org/10.1093/bioinformatics/btg405.
43. **Breitling R, Armengaud P, Amtmann A, Herzyk P.** 2004. Rank products: a simple, yet powerful, new method to detect differentially regulated genes in replicated microarray experiments. FEBS Lett. **573:**83–92. http://dx.doi.org/10.1016/j.febslet.2004.07.055.
44. **Saeed AI, Bhagabati NK, Braisted JC, Liang W, Sharov V, Howe EA, Li J, Thiagarajan M, White JA, Quackenbush J.** 2006. TM4 microarray software suite. Methods Enzymol. **411:**134–193. http://dx.doi.org/10.1016/S0076-6879(06)11009-5.
45. **Castillo-Davis CI, Hartl DL.** 2003. GeneMerge—post-genomic analysis, data mining, and hypothesis testing. Bioinformatics **19:**891–892. http://dx.doi.org/10.1093/bioinformatics/btg114.
46. **Kamau E, Meehan T, Lavine MD, Arrizabalaga G, Mustata Wilson G, Boyle J.** 2011. A novel benzodioxole-containing inhibitor of *Toxoplasma gondii* growth alters the parasite cell cycle. Antimicrob. Agents Chemother. **55:**5438–5451. http://dx.doi.org/10.1128/AAC.00455-11.
47. **Pavlidis P, Noble WS.** 2001. Analysis of strain and regional variation in gene expression in mouse brain. Genome Biol. **2:**RESEARCH0042. http://dx.doi.org/10.1186/gb-2001-2-10-research0042.
48. **Grigg ME, Ganatra J, Boothroyd JC, Margolis TP.** 2001. Unusual abundance of atypical strains associated with human ocular toxoplasmosis. J. Infect. Dis. **184:**633–639. http://dx.doi.org/10.1086/322800.
49. **Sibley LD, Boothroyd JC.** 1992. Virulent strains of *Toxoplasma gondii* comprise a single clonal lineage. Nature **359:**82–85. http://dx.doi.org/10.1038/359082a0.
50. **Khan A, Dubey JP, Su C, Ajioka JW, Rosenthal BM, Sibley LD.** 2011. Genetic analyses of atypical *Toxoplasma gondii* strains reveal a fourth clonal lineage in North America. Int. J. Parasitol. **41:**645–655. http://dx.doi.org/10.1016/j.ijpara.2011.01.005.
51. **Saeij JP, Boyle JP, Boothroyd JC.** 2005. Differences among the three major strains of *Toxoplasma gondii* and their specific interactions with the infected host. Trends Parasitol. **21:**476–481. http://dx.doi.org/10.1016/j.pt.2005.08.001.
52. **Boyle JP, Rajasekar B, Saeij JP, Ajioka JW, Berriman M, Paulsen I, Roos DS, Sibley LD, White MW, Boothroyd JC.** 2006. Just one cross appears capable of dramatically altering the population biology of a eukaryotic pathogen like *Toxoplasma gondii*. Proc. Natl. Acad. Sci. U. S. A. **103:**10514–10519. http://dx.doi.org/10.1073/pnas.0510319103.
53. **Ong YC, Reese ML, Boothroyd JC.** 2010. *Toxoplasma* rhoptry protein 16 (ROP16) subverts host function by direct tyrosine phosphorylation of STAT6. J. Biol. Chem. **285:**28731–28740. http://dx.doi.org/10.1074/jbc.M110.112359.
54. **Yamamoto M, Standley DM, Takashima S, Saiga H, Okuyama M, Kayama H, Kubo E, Ito H, Takaura M, Matsuda T, Soldati-Favre D, Takeda K.** 2009. A single polymorphic amino acid on *Toxoplasma gondii* kinase ROP16 determines the direct and strain-specific activation of Stat3. J. Exp. Med. **206:**2747–2760. http://dx.doi.org/10.1084/jem.20091703.
55. **Sibley LD, Niesman IR, Parmley SF, Cesbron-Delauw MF.** 1995. Regulated secretion of multi-lamellar vesicles leads to formation of a tubulovesicular network in host-cell vacuoles occupied by *Toxoplasma gondii*. J. Cell Sci. **108**(Part 4)**:**1669–1677.
56. **Kosugi S, Hasebe M, Matsumura N, Takashima H, Miyamoto-Sato E, Tomita M, Yanagawa H.** 2009. Six classes of nuclear localization signals specific to different binding grooves of importin alpha. J. Biol. Chem. **284:**478–485. http://dx.doi.org/10.1074/jbc.M807017200.
57. **Schares G, Meyer J, Barwald A, Conraths FJ, Riebe R, Bohne W, Rohn K, Peters M.** 2003. A Hammondia-like parasite from the European fox (Vulpes vulpes) forms biologically viable tissue cysts in cell culture. Int. J. Parasitol. **33:**229–234. http://dx.doi.org/10.1016/S0020-7519(03)00009-2.
58. **Gjerde B, Dahlgren SS.** 2011. Hammondia triffittae n. comb. of foxes (Vulpes spp.): biological and molecular characteristics and differentiation from Hammondia heydorni of dogs. Parasitology **138:**303–321. http://dx.doi.org/10.1017/S0031182010001265.
59. **Frenkel JK, Dubey JP.** 1975. *Hammondia hammondi*: a new coccidium of cats producing cysts in muscle of other mammals. Science **189:**222–224. http://dx.doi.org/10.1126/science.806116.
60. **Jerome ME, Radke JR, Bohne W, Roos DS, White MW.** 1998. *Toxoplasma gondii* bradyzoites form spontaneously during sporozoite-initiated development. Infect. Immun. **66:**4838–4844.
61. **Radke JB, Lucas O, De Silva EK, Ma Y, Sullivan WJ, Jr, Weiss LM, Llinas M, White MW.** 2013. ApiAP2 transcription factor restricts development of the *Toxoplasma* tissue cyst. Proc. Natl. Acad. Sci. U. S. A. **110:**6871–6876. http://dx.doi.org/10.1073/pnas.1300059110.
62. **Behnke MS, Wootton JC, Lehmann MM, Radke JB, Lucas O, Nawas J, Sibley LD, White MW.** 2010. Coordinated progression through two subtranscriptomes underlies the tachyzoite cycle of *Toxoplasma gondii*. PLoS One **5:**e12354. http://dx.doi.org/10.1371/journal.pone.0012354.
63. **Walker R, Gissot M, Croken MM, Huot L, Hot D, Kim K, Tomavo S.** 2013. The *Toxoplasma* nuclear factor TgAP2XI-4 controls bradyzoite gene expression and cyst formation. Mol. Microbiol. **87:**641–655. http://dx.doi.org/10.1111/mmi.12121.
64. **Radke JR, Behnke MS, Mackey AJ, Radke JB, Roos DS, White MW.** 2005. The transcriptome of *Toxoplasma gondii*. BMC Biol. **3:**26. http://dx.doi.org/10.1186/1741-7007-3-26.
65. **Reid AJ, Vermont SJ, Cotton JA, Harris D, Hill-Cawthorne GA, Konen-Waisman S, Latham SM, Mourier T, Norton R, Quail MA, Sanders M, Shanmugam D, Sohal A, Wasmuth JD, Brunk B, Grigg ME, Howard JC, Parkinson J, Roos DS, Trees AJ, Berriman M, Pain A, Wastling JM.** 2012. Comparative genomics of the apicomplexan parasites *Toxoplasma gondii* and *Neospora caninum*: coccidia differing in host range and transmission strategy. PLoS Pathog. **8:**e1002567. http://dx.doi.org/10.1371/journal.ppat.1002567.